Cardiac side population cells have a potential to migrate and differentiate into cardiomyocytes in vitro and in vivo

Tomomi Oyama,[1] Toshio Nagai,[1] Hiroshi Wada,[1] Atsuhiko Thomas Naito,[1] Katsuhisa Matsuura,[1] Koji Iwanaga,[1] Toshinao Takahashi,[1] Motohiro Goto,[1] Yoko Mikami,[1] Noritaka Yasuda,[1] Hiroshi Akazawa,[1] Akiyoshi Uezumi,[2] Shin'ichi Takeda,[3] and Issei Komuro[1]

[1]Department of Cardiovascular Science and Medicine, Chiba University Graduate School of Medicine, Chuo-ku, Chiba-shi, Chiba 260-8670, Japan
[2]Division for Therapies against Intractable Diseases, Institute for Comprehensive Medical Science, Fujita Health University, Kutsukake-cho, Toyoake, Aichi 470-1192, Japan
[3]Department of Molecular Therapy, National Institute of Neuroscience, National Center of Neurology and Psychiatry, Kodaira, Tokyo 187-8502, Japan

Side population (SP) cells, which can be identified by their ability to exclude Hoechst 33342 dye, are one of the candidates for somatic stem cells. Although bone marrow SP cells are known to be long-term repopulating hematopoietic stem cells, there is little information about the characteristics of cardiac SP cells (CSPs). When cultured CSPs from neonatal rat hearts were treated with oxytocin or trichostatin A, some CSPs expressed cardiac-specific genes and proteins and showed spontaneous beating.

When green fluorescent protein–positive CSPs were intravenously infused into adult rats, many more ($\sim$12-fold) CSPs were migrated and homed in injured heart than in normal heart. CSPs in injured heart differentiated into cardiomyocytes, endothelial cells, or smooth muscle cells (4.4%, 6.7%, and 29% of total CSP-derived cells, respectively). These results suggest that CSPs are intrinsic cardiac stem cells and involved in the regeneration of diseased hearts.

Introduction

Cardiomyocytes are thought to terminally differentiate and withdraw from the cell cycle after birth. Therefore, cardiac injury causes permanent myocardial loss and results in cardiac dysfunction (Colucci, 1997; Towbin and Bowles, 2002). However, three research groups, including ours, have recently reported the isolation of cardiac stemlike cells based on the two distinct cell surface antigens, such as stem cell antigen 1 (Sca-1; Oh et al., 2003; Matsuura et al., 2004) and c-kit (Beltrami et al., 2003). More recently, islet-1–positive cells have been reported to be a distinct population of cardiac progenitors in the postnatal heart, although the most of them do not contribute to the formation of the left ventricle and their existence in the adult heart is still unclear (Cai et al., 2003; Laugwitz et al., 2005).

When these primitive cells were cultured under appropriate conditions, the cells expressed cardiac proteins (Oh et al., 2003; Beltrami et al., 2003; Matsuura et al., 2004) and exhibited spontaneous beating (Matsuura et al., 2004). When transplanted into injured hearts, the cells differentiated into cardiomyocytes (Oh et al., 2003; Beltrami et al., 2003) and cardiac function was improved (Beltrami et al., 2003). Although it is still unclear whether these primitive cells fit the precise definition of stem cells, e.g., self-renewal capacity and reconstitutive capability of the total organ, these findings suggest that the heart has intrinsic stemlike cells, which may participate in its regeneration.

Side population (SP) cells are first identified as mouse hematopoietic stem cells with long-term multilineage reconstitution abilities based on their unique ability to efflux the DNA-binding dye Hoechst 33342 (Goodell et al., 1996, 1997). SP cells exist in a variety of organs, such as bone marrow, skeletal muscle, liver, brain, lung, skin, and heart (Asakura and Rudnicki, 2002; Montanaro et al., 2003). Zhou et al. (2001) reported that the ATP-binding cassette transporter, ABCG2 (also known as breast cancer resistance protein 1 [Bcrp1]), is a molecular determinant of this SP phenotype in hematopoietic stem cells. In mouse lung and rat liver, the SP phenotype has been reported to be largely determined by the expression of ABCG2

(Shimano et al., 2003; Summer et al., 2003). Among the tissue-derived SP cells, bone marrow and skeletal muscle SP cells have been well investigated. Bone marrow SP cells were first identified as a primitive population of hematopoietic stem cells (Goodell et al., 1996). The bone marrow–derived SP cells show long-term multilineage reconstitution in lethally irradiated recipients and form hematopoietic colonies in vitro (Goodell et al., 1996, 1997; Asakura and Rudnicki, 2002). Jackson et al. (2001) have reported that bone marrow SP cells also differentiate into endothelial cells and cardiomyocytes in ischemic hearts. Gussoni et al. (1999) reported that transplantation of skeletal muscle SP cells into the irradiated mdx mouse results in the reconstitution of the hematopoietic compartment of the transplanted recipients and regeneration of donor-derived, dystrophin-positive muscle in the affected muscle. Skeletal muscle SP cells have the in vitro hematopoietic activity, and differentiate into skeletal myocytes when cocultured with satellite cell–derived myoblasts (Asakura et al., 2002). These results suggest that SP cells have features of somatic stem cells, and that cardiac SP cells (CSPs) may be a promising candidate for cardiac stem/progenitor cells.

CSPs from postnatal hearts have been reported to differentiate into cardiomyocytes when cocultured with cardiomyocytes (Hierlihy et al., 2002; Martin et al., 2004; Pfister et al., 2005). However, factors that induce differentiation of CSPs into cardiomyocytes have not been identified. Several growth or humoral factors have been reported to possess the ability to induce the differentiation of primitive cells into cardiomyocytes. During the development, bone morphogenetic proteins (BMPs) and fibroblast growth factors promote cardiogenesis in chick (Sugi and Lough, 1995; Schultheiss et al., 1997). Both canonical and noncanonical Wnts play an important role in the cardiac differentiation (Eisenberg et al., 1997; Pandur et al., 2002; Naito et al., 2003). Oxytocin (OT) and dynorphin B induce differentiation of embryonic stem cells and P19 embryonal carcinoma cells into cardiomyocytes (Ventura and Maioli, 2000; Paquin et al., 2002; Ventura et al., 2003). Besides growth or humoral factors, chemical compounds such as DMSO and 5′-azacytidine have been reported to promote the cardiomyocyte differentiation of embryonic or somatic stem cells (Makino et al., 1999; Xu et al., 2002). These findings suggest that both extracellular signals and epigenetic modification are capable of turning the fate of stem cells to cardiomyocytes. Recently, Linke et al. (2005) have reported that c-kit–, MDR-1–, or Sca-1–positive cardiac stem cells migrate and proliferate in response to hepatocyte growth factor and insulin-like growth factor-1, respectively. However, it is still elusive whether CSPs, by responding to the ischemia-induced factors, move to the injured area of the heart and differentiate into cardiomyocytes.

We first report that CSPs from postnatal rat hearts differentiate into cardiomyocytes both in vitro and in vivo. Both OT and trichostatin A (TSA) induced postnatal CSPs to differentiate
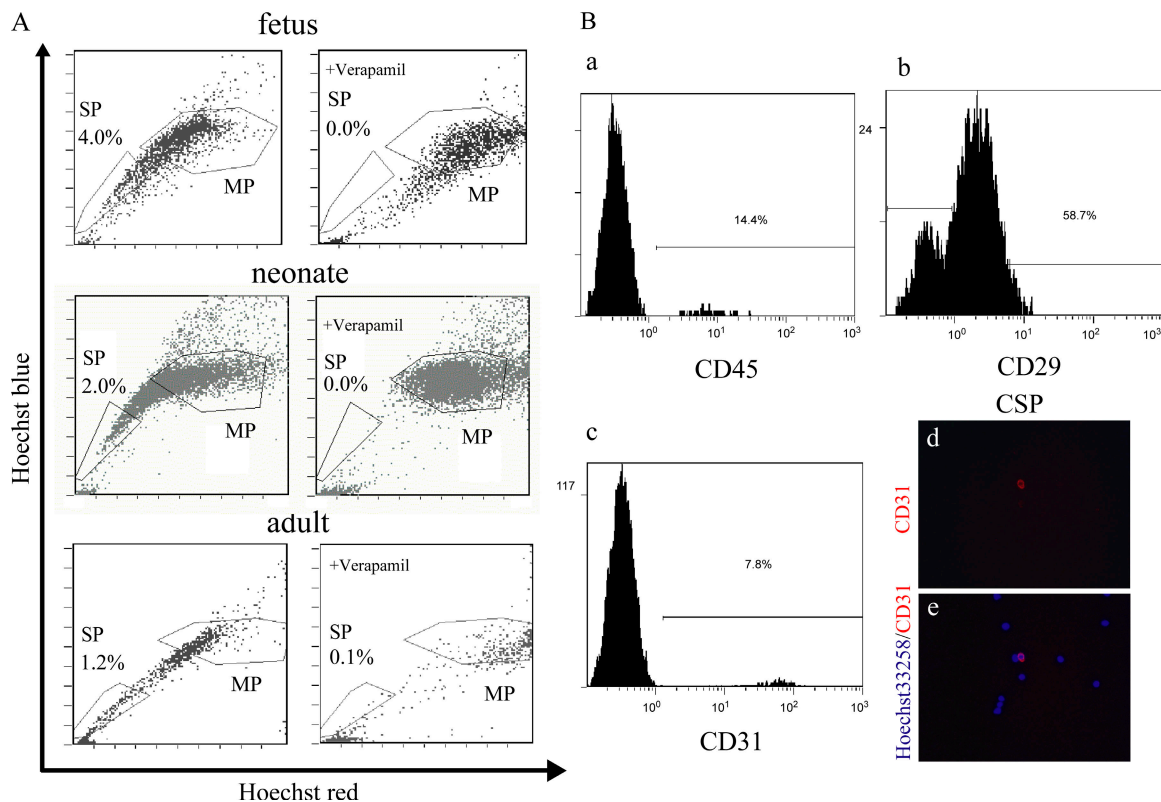

Figure 1. **Isolation of CSPs from rat hearts at the various developmental stages and characterization of CSPs from neonatal rat hearts.** (A) Flow cytometric analysis revealed that ~4% of SP cells exist in a cell suspension after isolation from fetal rat hearts, ~2% from neonatal rat hearts, and ~1.2% from adult rat hearts. There was no SP cell fraction after the treatment with verapamil. (B) Cell surface marker antigen analysis of CSPs. In CSPs, ~14% of the cells expressed CD45 (a), ~59% expressed CD29 (b) and ~8% expressed CD31 (c). Immunofluorescent images revealed that the percentage of CD31+ CSPs (d, red) in the total cells (e, blue) is almost identical with the result of flow cytometry.

into beating cardiomyocytes. After intravenous transplantation of CSPs into normal adult rats, CSPs migrated and homed in the interstitial space of myocardium. When CSPs were intravenously transplanted into the cryoinjured heart, the number of CSPs was significantly larger in the border area than in the remote or infarct area after transplantation. Furthermore, CSPs differentiated into cardiomyocytes, endothelial cells, or smooth muscle cells in the border area. These findings suggest that CSPs are resident cardiac stem cells, which can migrate and regenerate myocardium in response to the ischemia-induced factors.

Results

## Character of SP cells from postnatal hearts

Fluorescent sorting analysis revealed that there were two populations of cells in fetal, neonatal, and adult rat hearts referred to the SP and the main population (MP) cells in bone marrow (Fig. 1 A). When the cells were incubated with 50 μM verapamil, which is an inhibitor of multidrug resistance (MDR) and MDR-like proteins, there was no SP, suggesting that rat hearts contain SP cells. The proportion of CSP in the total cardiac-derived cells was ∼4.0%, ∼2.0%, and 1.2% in fetal, neonatal, and adult hearts, respectively. In neonatal CSPs, ∼14% of the cells expressed CD45, ∼59% expressed CD29, and ∼8% expressed CD31 (Fig. 1 B, a–c). The percentage of CD31-positive cells was 13.1 ± 4.0% under the fluorescent microscope (Fig. 1 B, d and e). To examine whether CSPs were in a non-cycling quiescent state, cardiac cells were stained with both Hoechst 33342 and Pyronin Y (PY). The percentage of cells in PY-negative G0 stage was significantly higher in CSPs (74.3 ± 1.4%) than in cardiac MP cells (CMP; 34.0 ± 2.6%; Fig. 2 A, a). A comparable result was obtained from the bone marrow SP and MP cells (PY-negative G0 stage of bone marrow SP, 79.8 ± 3.1%; bone marrow MP, 41.7 ± 5.4%; Fig. 2 A, b). This suggests that CSPs represent a quiescent stem cell population in the heart.

We next examined whether cardiac SP cells express Bcrp1, the molecular determinant of the SP phenotype. RT-PCR analysis showed that the Bcrp1 gene was expressed in freshly isolated SP cells from neonatal rat hearts, as well as in those from mouse bone marrow, but not in MP cells of hearts and of bone marrow (Fig. 2 B). Immunostaining with anti-Bcrp1 antibody revealed that Bcrp1 protein was detected on the cell surface of CSP, as well as bone marrow SP cells, but not in the MP cells (Fig. 2 C).

Localization of CSP in the heart

In neonatal rat hearts, most Bcrp1-positive cells (∼95.4%) were CD31 (Fig. 3 A, a [coronary artery] and b [capillary]), but there were some CD31-negative/Bcrp1-positive cells (Fig. 3 A, c, arrowheads). Most of the CD31-negative/Bcrp1-positive cells (94.3 ± 9.8%) existed in the perivascular area (Fig. 3 A, c–e, arrowheads). There were also a few CD31-negative/Bcrp1-positive cells in the interstitial space (5.6 ± 9.8%; Fig. 3 A, f–i,
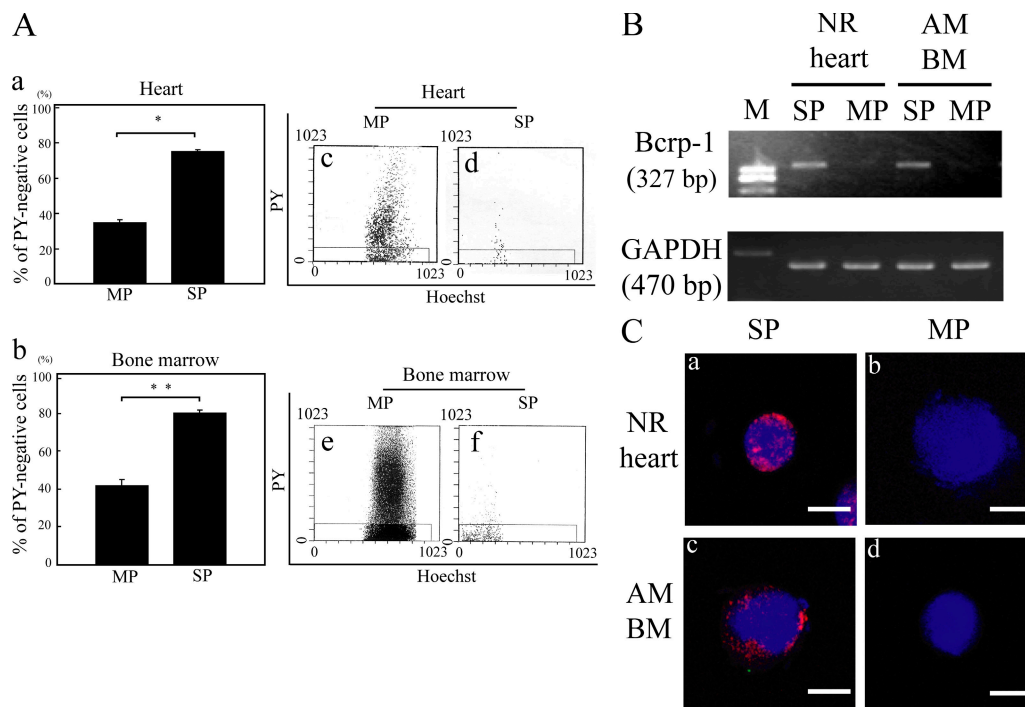
Figure 2. **Quiescence of CSPs and Bcrp1 mRNA and protein expression in CSPs.** (A) Quiescence properties of CSPs. Neonatal rat heart cells and adult mouse bone marrow cells were subdivided into SP and MP cells, respectively, and the incorporation of PY was analyzed (a). The data shown represent the mean ± the SD (*, P < 0.0001; **, P < 0.0005). Hoechst and PY staining emission pattern of CMP (c), CSPs (d), bone marrow MP (e), and bone marrow SP (f) were shown. (B) Expression of Bcrp1 mRNA in sorted SP cells and MP cells. Adult mouse bone marrow SP and MP cells were used as positive and negative controls. NR, neonatal rat; AM, adult mouse; BM, bone marrow; M, molecular weight marker (100 bp ladder). (C) Bcrp1 protein expression in SP cells and MP cells. Confocal images revealed expression of Bcrp1 on the surface of the cardiac SP cells (a, in red), as well as bone marrow SP cells (c, in red) but not on cardiac (b) and bone marrow (d) MP cells. Nuclei were stained with TOPRO-3 and shown in blue. Bars, 5 μm.
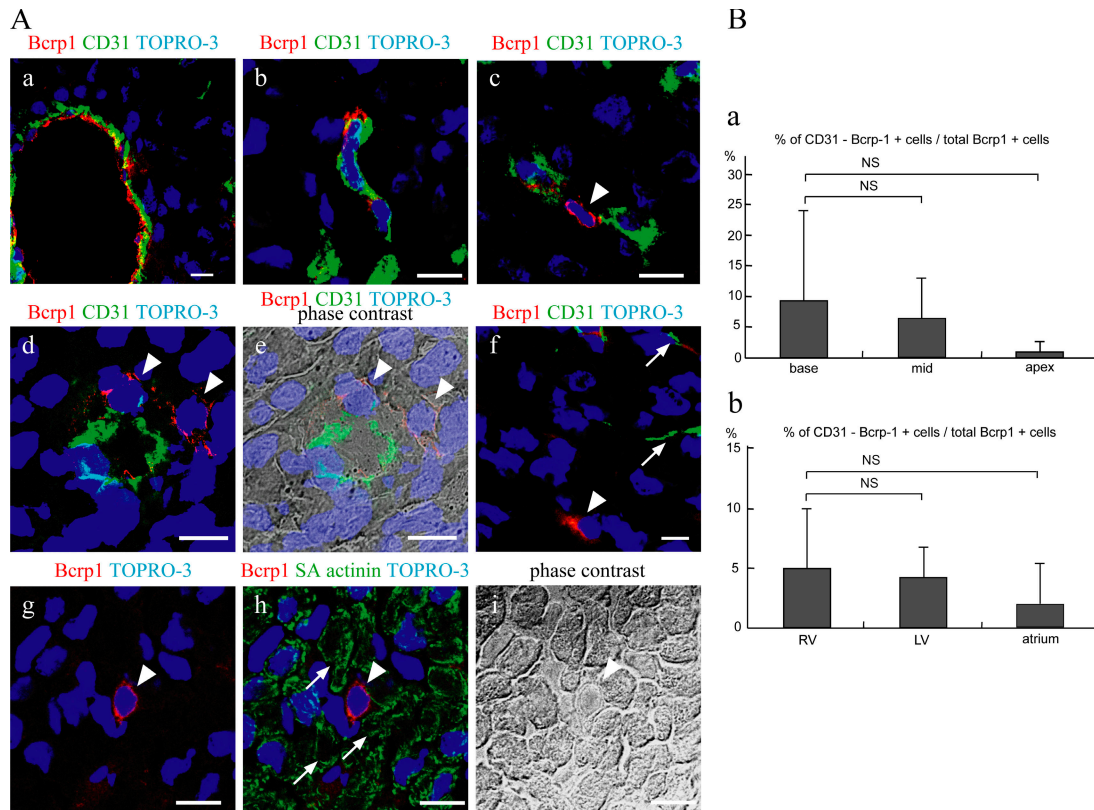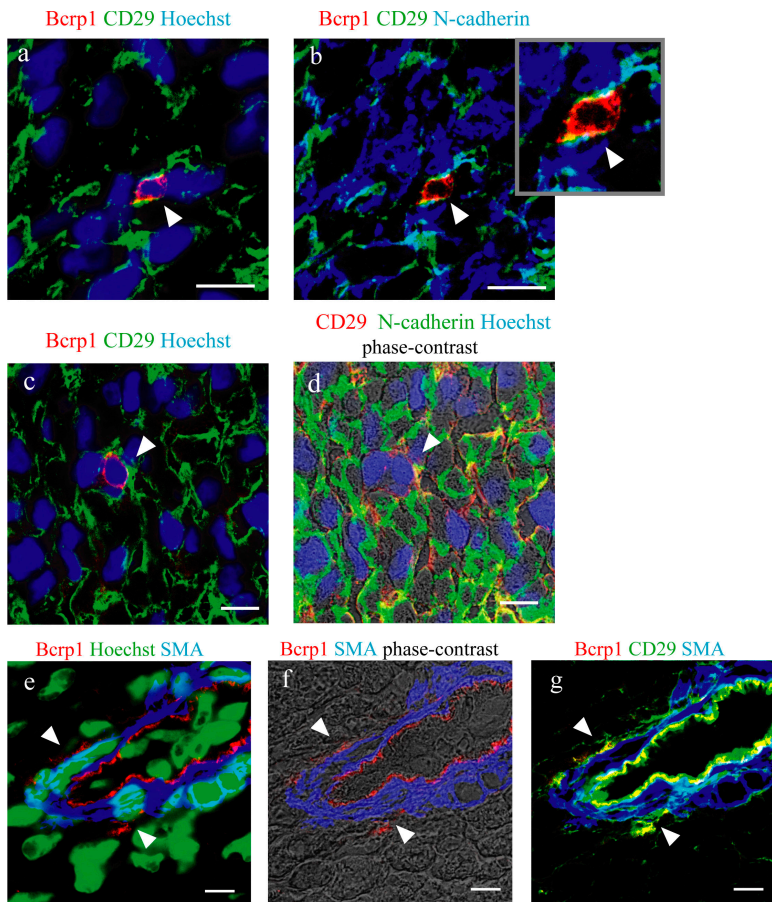
Figure 3. **Distribution of CSPs in neonatal rat hearts.** (A) The expression of Bcrp1 and CD31 in the neonatal rat hearts. Bcrp1 expression was detected in the endothelium of arteriole and capillary, which coexpressed CD31 (a–c; red, Bcrp1; green, CD31; blue, nucleus). A CD31-negative/Bcrp1-positive cell was observed (c, arrowhead). Typical examples of perivascular CSPs (arrowhead in d and e; Bcrp1 in red, CD31 in green and nucleus in blue, e; a phase-contrast image was overlaid on d) and an interstitial nonperivascular CSP (f–i, arrowhead; red, Bcrp1; blue, nucleus). Arrows indicate CD31 in f and SA in h. Bars, 10 μm. (B) Quantitative analysis of the distribution of CSPs. Total 713 Bcrp1-positive cells in the sections from three neonatal rat hearts were evaluated. (a and b) Percentage of CD31-negative/Bcrp1-positive cells/total Bcrp1-positive cells in the different portions in left ventricles (a) and the different chambers (b). A section of left ventricle was divided into three equal lesions (base, mid, and apex), along with a long axis. The data shown represent the mean $\pm$ the SD.

arrowheads) between cardiomyocytes, which were stained with sarcomeric α-actinin (SA; Fig. 3 A, h, arrows) and distant from CD31-positive vessels (Fig. 3 A, f, arrows). There were no significant differences in the percentage of CD31-negative/Bcrp1-positive cells per total Bcrp1-positive cells among apex, mid, and base of left ventricles (Fig. 3 B, a), and also among chambers (i.e., atrium, left, and right ventricles; Fig. 3 B, b). It has been reported that N-cadherin, CD29, and β1 integrin mediate the adhesion of stem cells to specialized mesenchymal cells and extracellular matrix in the niche environment (Zhang et al., 2003; Wilson et al., 2004). Bcrp1-positive cells in the interstitial space coexpressed CD29 and N-cadherin around the surface of the cells (Fig. 4, a and b, arrowheads). At the junction of Bcrp1-positive cells and the neighboring cell, abundant coexpression of CD29 and N-cadherin was observed (Fig. 4, c and d, arrowheads). The perivascular Bcrp1-positive cells, which were localized adjacent to the smooth muscle cell actin (SMA)–positive cells, coexpressed CD29 (Fig. 4, e–g, arrowheads). These findings suggest that Bcrp1-positive cardiac stem or progenitor cells were localized in the specialized area of the myocardium, which may be similar to the stem cell niche in other organs, such as hematopoietic and gonad systems (Gonzalez-Reyes, 2003; Zhang et al., 2003; Wilson et al., 2004).

CSPs differentiate into cardiomyocytes in vitro

Isolated CSPs attached to the gelatin-coated dishes by 24 h with medium containing FBS. To induce differentiation into cardiomyocytes, we cultured CSPs with various growth factors, such as BMP2, BMP4, and OT, or on the feeder layers of the mesenchymal cells. Only treatment with OT was able to induce CSP into beating cardiomyocytes. After 2 d of treatment with OT, CSPs started to show various cell shapes (Fig. 5 A, a). 10 d after treatment, the attached cells started to proliferate, and elongated spindle-shaped cells became predominant (Fig. 5 A, b). 3 wk after treatment, some clusters of beating cells were recognized among flattened cells (Fig. 5 A, c and Video 1, available at http://www.jcb.org/cgi/content/full/jcb.200603014/DC1). Next, we examined whether methylation inhibitors or histone deacetylase inhibitors induced cardiac differentiation of CSPs. The treatment with TSA, but not with 5-azacytidine, induced CSPs into beating cardiomyocytes. The morphology of the CSPs treated with TSA was similar to that of CSPs treated with OT, although proliferation of the elongated spindle-shaped cells was less observed in the treatment with TSA compared with OT at ∼10 d (Fig. 5 A, d and e). 3 wk after the treatment, some clusters of beating cells were recognized among flattened cells

Bcrp1 CD29 Hoechst

Bcrp1 CD29 N-cadherin

Bcrp1 CD29 Hoechst

CD29 N-cadherin Hoechst
phase-contrast

Bcrp1 Hoechst SMA

Bcrp1 SMA phase-contrast

Bcrp1 CD29 SMA

Figure 4. **Expression of CD29 and N-cadherin in CSPs.** Interstitial Bcrp1-positive cells coexpressed CD29 (a and c, arrowhead; red, Bcrp1; green, CD29; blue, nuclei; yellow, coexpression of CD29 and Bcrp1). Coexpression of Bcrp1, CD29, and N-cadherin was shown in l b and the inlet as white, yellow, or light blue color, which was dependent on the degree of the expression of three distinct cell surface proteins. Spatial orientation of coexpression of CD29 and N-cadherin was shown in d, in which CD29 was colored in red, N-cadherin in green, and nuclei in blue; phase-contrast image was overlaid. An arrowhead in d indicates the identical Bcrp1-positive cell indicated in c. Perivascular Bcrp1-positive cells (arrowheads in e and f; red, Bcrp1; blue, SMA; and green, nuclei; phase-contrast image was overlaid on f) coexpressed CD29 (g, arrowhead; red, Bcrp1; green, CD29; and blue, SMA; yellow, coexpression of Bcrp1 and CD29). Bars, 10 μm

(Fig. 5 A, f, and Video 2). There were no differences between OT- and TSA-induced cardiomyocytes in regard to the percentage of beating cells (OT, $0.27 \pm 0.2\%$; TSA, $0.50 \pm 0.21\%$; Fig. 5 B, c, shaded bar) and the percentage of SA-positive cells (OT, $3.8 \pm 3.8\%$; TSA, $5.5 \pm 3.9\%$; Fig. 5 B, c, open bar). Low magnification immunofluorescent images of SA and nuclear DNA of OT- and TSA-induced cardiomyocytes are shown in Fig. 5 B (a [OT] and b [TSA]). Fine striation was observed in OT- and TSA-induced cardiomyocytes (Fig. S2 A, a–d). Nontreated SP cells never exhibited spindle-shaped morphology or beating, and MP cells treated with OT or TSA detached from culture dishes within 1 wk.

Next, we examined the gene expression of cardiac transcription factors and contractile proteins in CSPs by RT-PCR. Before treatment with OT or TSA, none of these cardiac genes were expressed (Fig. 5 C, P). Three weeks after treatment with OT or TSA, cardiac transcription factors, including *Nkx2.5*, *GATA4*, and *myocyte-enhancer factor 2C* (*MEF-2C*), and contractile proteins, such as β–myosin heavy chain and *myosin light chain 2v* (*MLC-2v*), were expressed (Fig. 5 C, OT and TSA). Treatment with 100 nM OT antagonist (OTA; [d(CH2)5-1,Tyr(Me)-2,Thr-4,Orn-8,Tyr-NH2-9] vasotocin) completely inhibited OT-induced expression of cardiac genes (Fig. 5 C, OT+OTA), indicating that OT induced cardiomyocyte differentiation through authentic OT receptors. Cardiac gene expression was not observed in cells cultured with vehicle (Fig. 5 C, V).

To examine the expression of cardiac proteins, the CSPs treated with OT or TSA were stained with specific antibodies against cardiac proteins. The cells treated with OT or TSA expressed GATA4 (Fig. 5 D, a and d), atrial natriuretic factor (ANF; Fig. 5 D, b, c, e, and f), cardiac troponin T (cTnT; Fig. 5 D, c and f), MLC2v (Fig. 5 D, a), and SA (Fig. 5 D, b, d, and e). Notably, staining of each contractile protein showed a fine striated pattern, suggesting that treatments with OT or TSA induced differentiation of CSPs into mature cardiomyocytes.

Cardiac SP cells can differentiate into osteocytes and adipocytes

It has been reported that SP cells from skeletal muscle and bone marrow differentiate into various types of cells, such as adipocytes, endothelial cells, and skeletal muscle and cardiac myocytes (Asakura et al., 2002; Iijima et al., 2003; Tamaki et al., 2003). To determine whether CSPs from the heart have multipotency of differentiation, we examined whether these cells could differentiate into cells other than cardiomyocytes. When CSPs were cultured with osteogenic inducers, including β-glycerophosphate, dexamethasone, and ascorbic acid-2 phosphate, some SP cells stained positive with alkaline phosphatase, which is one of the early markers of osteocytes (Fig. S1 A, a, available at http://www.jcb.org/cgi/content/full/jcb.200603014/DC1). RT-PCR analysis revealed that expression of alkaline phosphatase gene was induced in cardiac SP cells after treatment with osteogenic inducers (Fig. S1 A, b, lane O). On the other hand,
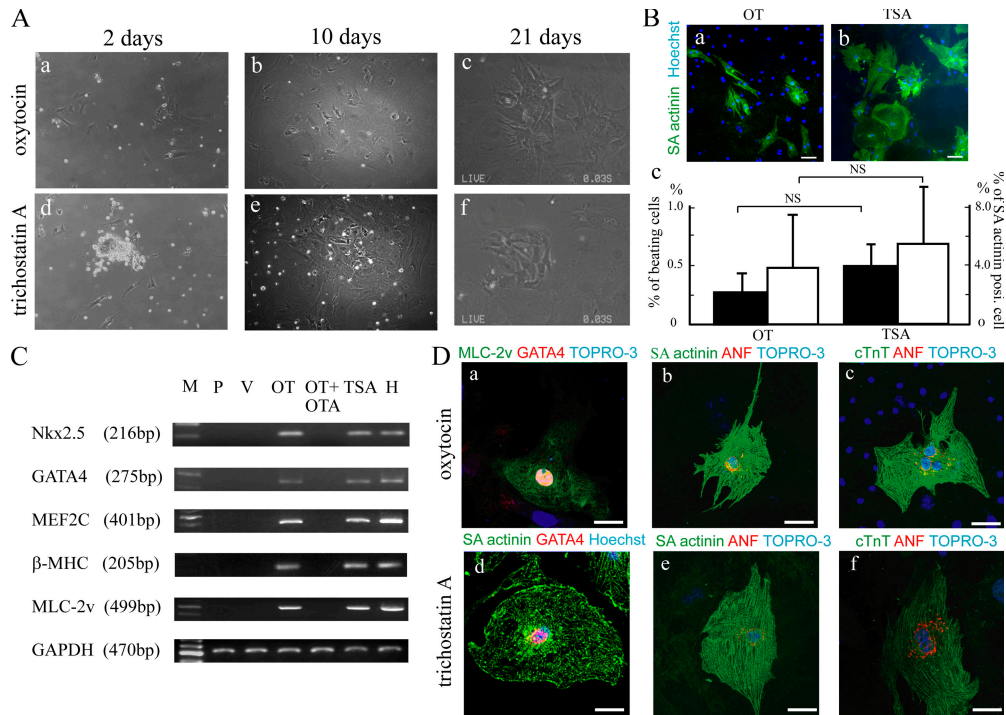
Figure 5. **Differentiation of CSPs into beating cardiomyocytes.** (A) Phase-contrast images of CSPs after treatment with OT (a–c) and TSA (d–f). 2 d after treatment with OT and TSA, CSPs slowly attached to the culture dishes (a, OT; d, TSA), proliferated rapidly after 10 d (b, OT; e, TSA), and started beating after 21 d (c, OT; f, TSA). Movies of beating CSP-derived cardiomyocytes are presented in Videos 1 and 2. (B) Quantitative analysis of the percentage of beating and SA-positive cells in CSPs treated with OT and TSA After counting the number of beating cells, the cells were immunostained with SA and Hoechst dye (a OT, b TSA). The percentage of beating and SA-positive cells in total nuclei was shown in c. The data shown represents the mean ± the SD of four to seven samples from three independent experiments. (C) Expression of cardiac protein mRNA in CSPs treated with OT or TSA. Total RNA obtained from the neonatal rat heart was used as positive controls (lane H). Loading of equal amounts of RNA was confirmed by expression of the GAPDH gene. P, pretreatment; V, vehicles; OTA, OT receptor antagonist; M, molecular weight marker (100-bp ladder). (D) Expression of cardiac proteins in CSPs after treatment with OT (a–c) or TSA (d–f). a and b, GATA4 (red); b, d, and e, SA (green); b, c, e, and f ANF (red); c and f, cTnT (green); a MLC-2v, (green). Nuclei were stained with TOPRO-3 (blue). Videos 1 and 2 are available at http://www.jcb.org/cgi/content/full/jcb.200603014/DC1. Bars: (B) 20 μm; (D) 10 μm.

cardiac SP cells treated with OT or TSA did not express alkaline phosphatase (Fig. S1 A, b, lanes OT and T). When cardiac SP cells were cultured in adipogenic induction with MDI-I mixture for 20 d, some SP cells showed cytoplasmic accumulation of oil droplets stained with Oil Red O, indicating that CSPs differentiated into adipocytes (Fig. S1 A, c).

CSPs migrate and home into the injured heart

When GFP$^+$ CSPs were transplanted into the normal rat via the tail vein, GFP$^+$ CSPs were distributed over the various organs, such as lung (Fig. 6 A, a), spleen (Fig. 6 A, b), liver (Fig. 6 A, c and d), skeletal muscle (Fig. 6 A, e and f), bone marrow (Fig. 6 A, g and h), and heart (Fig. 6 A, i–l). In the lung and spleen, there were less GFP$^+$ cells at 12 wk than at 1 wk after transplantation (12 wk/1 wk ratio; 0.19 for lung and 0.67 for spleen; Fig. 6 B). On the contrary, in the liver, skeletal muscle, and heart, more GFP$^+$ cells existed at 12 wk than at 1 wk after transplantation (12 wk/1 wk ratio; 1.63 for liver, 2.0 for skeletal muscle, and 3.0 for heart; Fig. 6 B). 4 wk after transplantation, some GFP$^+$ CSPs in the liver expressed albumin (Fig. 6 A, c and d). In skeletal muscle, GFP$^+$ CSPs had multiple nuclei and expressed desmin (Fig. 6 A, e and f). However, there were no GFP$^+$ CSPs positive for CD45 in the bone marrow (Fig. 6 A,

g and h). GFP$^+$ CSPs in the heart expressed CD29 (Fig. 6 A, i and j) and were localized in the interstitial space of myocardium, which was delineated by collagen type IV (Fig. 6 A, k and l). In the normal heart, transplanted GFP$^+$ CSPs did not express cTnT (not depicted).

Next, we examined whether myocardial injury facilitates migration and homing of transplanted GFP$^+$ CSP- and CMP-derived cells into the heart. 4 wk after transplantation of CMP, there were very few GFP$^+$ CMPs in both normal and injured hearts (Fig. 7 A, a and b). In CSP-transplanted rat hearts, there were a few GFP$^+$ CSPs, even in the normal myocardium (Fig. 7 A, c, arrowheads), whereas many GFP$^+$ CSPs existed in the injured heart (Fig. 7 A, d, arrowheads). Many more GFP$^+$ CSPs existed in the cryoinjured heart (15.0 ± 6.2 per 10^4 cells; $n = 3$) in comparison with the normal heart (1.3 ± 1.0 per 10^4 cells; $n = 3$; Fig. 7 A) 4 wk after transplantation. There was no substantial difference in the number of GFP$^+$ CMPs between normal (0.3 ± 0.6 per 10^4 cells; $n = 3$) and cryoinjured heart (0.7 ± 0.6 per 10^4 cells; $n = 3$; Fig. 7 A). GFP$^+$ CSPs were more abundant in the border zone of injured hearts (12.5 ± 2.5% of total cells) than in the normal (4.8 ± 1.4%) or injured (5.2 ± 1.7%) area (Fig. 7 B). Some GFP$^+$ CSPs in the border and injured area expressed cTnT (Fig. 8 A, a–d), vimentin (Fig. 8 A, e–h), von Willebrand factor (vWF; Fig. 8 A, i–l), and calponin
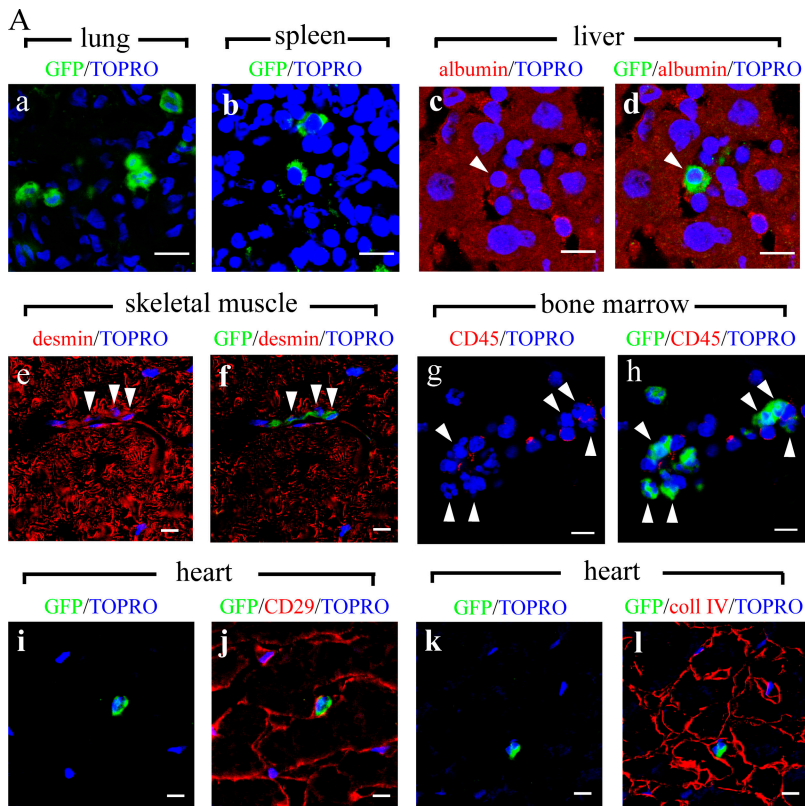
Figure 6. Tissue distribution of CSPs after intravenous transplantation. (A) CSPs distributed and resided in various organs 4 wk after intravenous infusion. GFP+ CSPs (green) in lung (a), spleen (b), liver (c and d), skeletal muscle (e and f), bone marrow (g and h), and heart (i–l). Arrowhead in c and d, GFP+ CSPs positive for albumin (red). Arrowheads in e and f, myotube-like GFP+ CSPs positive for desmin (red). Arrowheads in g and h, GFP+ CSPs negative for CD45 (red). CD29 and collagen type IV were represented in red in j and l. Nuclei were stained with TOPRO-3 (blue). Bars, 10 μm. (B) Fold increase of the number of GFP+ CSPs in the organs through 1 to 12 wk. The relative number of GFP+ CSP-derived cells in every organ at 1 wk is 1.0.
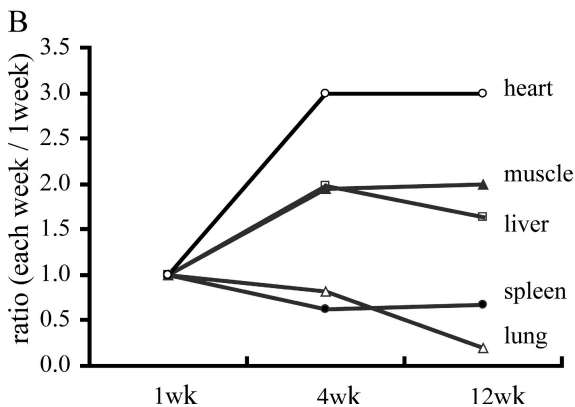
(Fig. 8 A, m–p). The percentage of cTnT-positive GFP+ cells in the total GFP+ cells was 4.4%, vimentin-positive GFP+ cells 33%, vWF-positive GFP+ cells 6.7%, and calponin-positive GFP+ cells 29% (Fig. 8 B). The SA-actinin–positive GFP+ cells (8.6%; $n = 56$) showed fine striated sarcomere structure. The majority of SA-positive CSPs were small cells without organized sarcomere structure (Fig. S2 B, a, arrowheads), suggesting that these cells remain in the stage of immature cardiomyocytes or cardiac precursor cells. There were some well-differentiated cardiomyocytes (Fig. S2 B, b, c, and d, arrowheads). Among the SA-positive GFP+ cells we examined, only a few small cells contained multi-nuclei without striation (Fig. S2 B, e and f, arrowheads). Small cell size and premature structure of this multinucleated cell suggest that the cell of multinuclei comes from mitosis rather than cell fusion. CSPs in the normal area of the injured heart did not express any of the aforementioned markers. These findings suggest that the injured myocardium recruits circulating CSPs, but not CMP, to the heart and stimulates the migration of CSPs toward the injured area. Furthermore, some environmental cues from the injured heart induce the differentiation of CSPs into cardiomyocytes, fibroblasts, endothelial cells, and smooth muscle cells.

Discussion

The novelty of our findings can be summarized as follows. First, we showed that a single factor, OT or TSA, can induce differentiation of CSPs into beating cardiomyocytes, which is quite different from the findings of previous studies (Hierlihy et al., 2002; Martin et al., 2004; Pfister et al., 2005; Tomita et al., 2005). Previous studies used coculture method to induce differentiation. Because OT is a physiological hormone, our findings may lead to identification of the intrinsic signals for cardiomyocyte differentiation. Second, we showed the precise location

Figure 7. **Homing ability of intravenously transplanted CSPs in cryoinjured heart.** (A) CSPs exclusively migrate and home into injured heart. Normal CMP, CMP transplanted into normal heart; injured CMP, CMP transplanted into cryoinjured heart; normal CSPs, CSPs transplanted into normal heart; injured CSPs, CSPs transplanted into cryoinjured heart. The data shown represents the mean ± the SD. *, P < 0.05. (bottom) Confocal images stained with cTnT (red), GFP (green), and TOPRO-3 (blue) were presented as a (normal CMP), b (injured CMP), c (normal CSPs), and d (injured CSPs). Arrowheads indicate GFP+ CMPs or CSPs. Bars, 10 μm. (B) Distribution of CSPs in the cryoinjured heart. The number of GFP+ CSPs in the normal, border, and infarct area was counted and represented as the percentage of GFP+ CSPs per total cells in the section. The data shown represent the mean ± the SEM. *, P < 0.05.
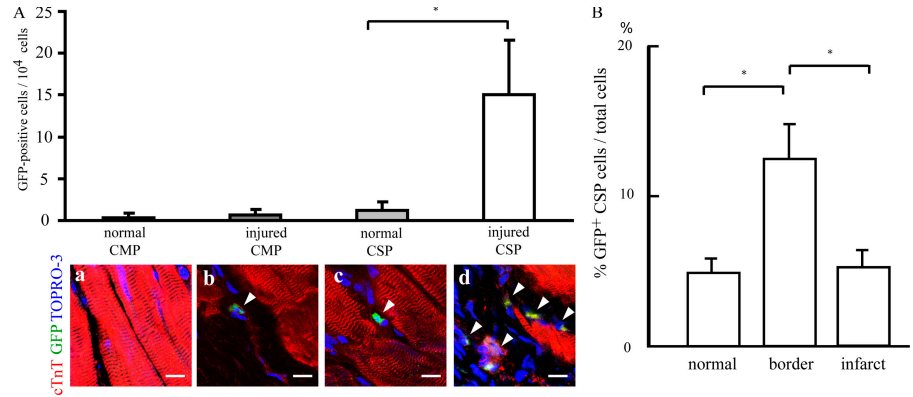
and distribution of CSPs in the heart. We distinguished CSPs from endothelial cells by immunohistochemical methods and clearly demonstrated the specific location of CSPs. Third, we demonstrated the expression of CD29 and N-cadherin on the cell surface of CSPs, suggesting that CSPs may be regulated in the niche in the heart. Fourth, we first demonstrated a sequential event of migration and homing of CSPs in the injured heart. There was no report concerning the in vivo dynamics of CSPs, and our findings suggest that the injured heart secrets some factors that recruit CSPs. Finally, we showed that transplanted CSPs followed the various steps of cardiomyogenesis, such as cardiac precursors and immature and mature cardiomyocytes. In addition, we showed that CSPs differentiate into multiple

cell lineages other than cardiomyocytes, including fibroblasts, endothelial cells, and smooth muscle cells.

Two groups have reported expression of cardiac proteins in CSPs when cocultured with primary cardiomyocytes (Hierlihy et al., 2002) or with CMP (Martin et al., 2004). Because both groups did not examine the contractile ability of SP-derived cells, it has remained unclear whether CSPs differentiate into mature cardiomyocytes. In addition, by the coculture method, it is difficult to distinguish if cardiomyocyte differentiation is accomplished by transdifferentiation or fusion. Recently, Pfister et al. (2005) that CD31-negative CSPs also differentiate into functionally beating cardiomyocytes by coculture with adult rat cardiomyocytes. In this study, we first demonstrated that
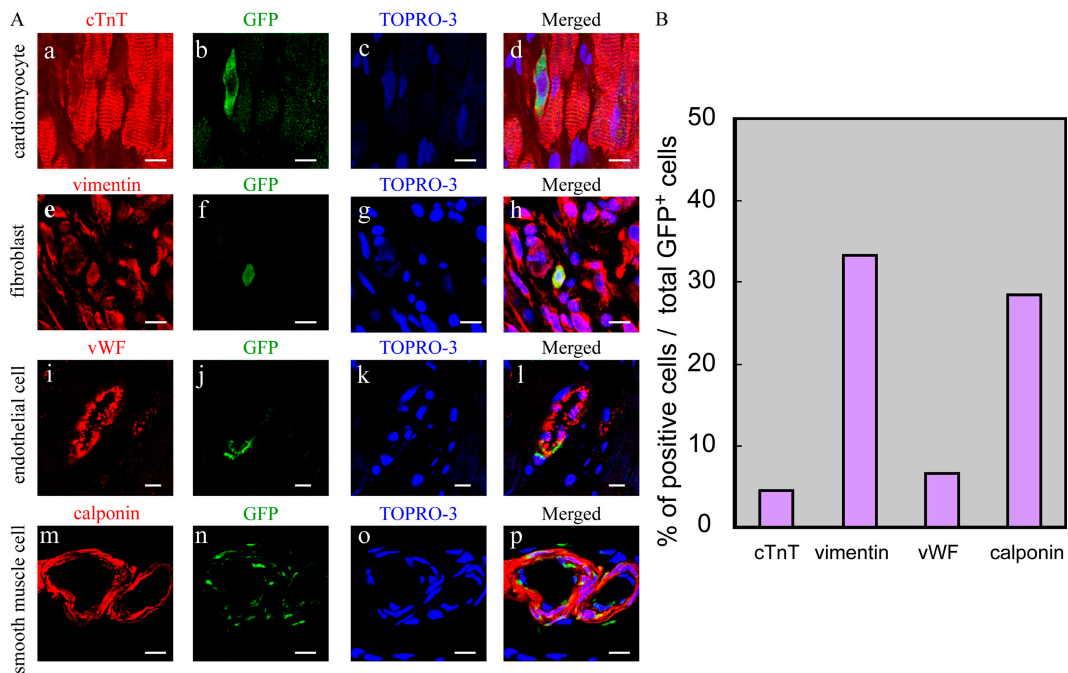
Figure 8. **Multilineage differentiation of CSPs.** (A) CSPs in the border area of the injured heart differentiate into various types of cells. GFP+ CSP-derived cells (b, f, j, n; green) expressed cTnT (a, red), vimentin (e, red), vWF (i, red), calponin (m, red). Nuclei were stained with TO-PRO-3 (blue). Merged images were represented in the right row. Bars, 10 μm. (B) Quantitative analysis of the frequency of expression of cell lineage marker proteins. The data were represented as the percentage of the expression of cTnT, vimentin, vWF, or calponin-positive cells per total GFP+ cells per section.

CSPs could differentiate into mature cardiomyocytes, which showed not only cardiac gene expression but also sarcomere formation and spontaneous beating, by single reagents such as OT and TSA.

There were more CSPs in the rat heart of the early developmental stage. Fetal rat CSPs account for ~4% of total isolated cells, 2% of neonatal rat CSPs, and 1.2% of adult rat CSPs. Our result of the developmental change of the CSP fraction is similar to the previously reported one in mouse hearts (Tomita et al., 2005). The percentage of CSPs from adult mouse was ~0.24% in our experiments (unpublished data). The percentage varied from 0.02% to 2% in previous reports (Hierlihy et al., 2002; Oh et al., 2003; Martin et al., 2004; Tomita et al., 2005). Although there may be a difference in the percentage of CSPs among the species, the cell surface markers of isolated CSPs were variable among the reports. Pfister et al. (2005) and Tomita et al. (2005) reported that a large portion of isolated CSPs from adult mouse are CD31 positive. In this study, CD31-positive cells were only 7.6% in isolated CSPs from neonatal rats. Our immunohistochemical analysis indicated that most Bcrp1-positive cells in the heart are CD31-positive endothelial cells. The reason for these variations may be attributed to distinct isolation techniques and to the fact that most endothelial cells were lost during the step of cell isolation discussed in this study. Considering the conclusion of Pfister et al. (2005) that CD31-negative CSPs represent a distinct cardiac progenitor cell population, our CSPs isolated from neonatal rats are a condensed population of cardiac progenitors.

The ability to induce CSPs into the mature cardiomyocytes is comparable between OT and TSA (Fig. 5 B). There were only a few studies showing quantitative analysis of the frequency of monocultured CSP-derived cardiomyocytes. Pfister et al. (2005) reported that ~10% of CD31$^-$/Sca-1$^+$/CSP expressed disorganized α-actinin and troponin I, but they did not show the characteristic sarcomeric organization and spontaneous beating, suggesting immature cardiomyocytes. Tomita et al. (2005) have reported that when CSP-derived cardiosphere was dissociated and cultured, 0.28% of the total cells differentiated into cardiomyocytes, which were positive for α-actinin and sarcomeric myosin (Tomita et al., 2005). In this study, ~5% of CSPs differentiated into cardiomyocytes with fine sarcomere structures and spontaneous beating (Fig. S2 A, a–f). Therefore, both OT and TSA possess more powerful cardiogenic activity against CSPs than the previously reported methods.

OT, a hypothalamic neuropeptide, induces uterine contraction and milk ejection. In recent years, however, functional OT receptors have been found in various organs, such as kidney, ovary, testis, thymus, heart, vascular endothelium, osteoclasts, myoblasts, pancreatic islet cells, adipocytes, and several types of cancer cells (Gimpl and Fahrenholz, 2001). OT receptors and OT biosynthesis are detected in atria and ventricles of the rat heart, and OT is thought to be involved in ANF release from cardiomyocytes (Gutkowska et al., 1997; Jankowski et al., 1998). CSPs are a heterogenous population of the cells, including cardiac stem/progenitor cells, endothelial progenitor cells, and other unknown cells. When CSPs are treated with OT or TSA, mesenchymal-like cells were observed near cardiomyocytes.

Presently, we do not have the evidence to indicate that OT receptors are expressed in cardiac stem/progenitor cells, but not in other cells. It has recently been reported that elevated OT and OT receptor protein levels in growing fetal hearts and OT receptor immunostaining were predominantly detected in cardiomyocytes and endothelial cells (Jankowski et al., 2004). These observations suggest that OT acts on cardiomyogenesis, but it remains to be determined whether OT has direct effects on cardiac stem cells.

We have recently reported that OT induces differentiation of adult cardiac Sca-1 cells into mature cardiomyocytes (Matsuura et al., 2004). Because of the lack of Sca-1 in rats and the unavailability of decent antibodies against rat c-kit, we could not determine the relationship between CSPs and other cardiac stem cells populations, such as Sca-1$^+$ or c-kit$^+$ cells. The expression of cardiac transcription factors was absent in freshly isolated CSPs. We performed semiquantitative RT-PCR, showing the expression levels of *Nkx-2.5* in CSPs were negligible (Fig. S1C, a and b). Therefore, CSPs may be more primitive stem or progenitor cells in comparison with cardiac Sca-1$^+$ cells, in which faint but substantial expressions of cardiac transcription factors were observed. Our findings suggest that the OT-mediated signaling may play a pivotal role in the differentiation of various cardiac stem cells into cardiomyocytes.

Histone deacetylases (HDAC) catalyze the deacetylation from conserved lysine residues in the N-terminal tails of histones (Hassig and Schreiber, 1997). Silencing of genes has been shown to be accomplished by histone deacetylation, and inhibition of HDAC reverses the silencing effect. HDAC are critically involved in cell cycle regulation, cell proliferation, cancer development, and cell differentiation (Marks et al., 2003; Legube and Trouche, 2003). Recently, HDAC inhibitors such as TSA, valproic acid, and butyric acid have been reported to modulate cell type–specific gene expression. The lymphoid lineage-determining factor Ikaros is repressed under the circumstances with hypoacetylation of core histones at promoter sites, and this repression is relieved by TSA (Koipally et al., 1999). Hsieh et al. (2004) reported that valproic acid induces neural differentiation of adult hippocampal neural progenitors through the induction of neuroD. In this study, TSA induced de novo expressions of *Nkx2.5*, *GATA4*, and *MEF2C*, suggesting that acetylation of chromatin activates specific master genes, products of which promote the expression of a series of cardiac transcription factors. It remains to be determined what genes are activated and involved in cardiomyocyte differentiation by the treatment of TSA.

SP cells are thought to be a population of quiescent stem cells, which reside in the niche of the organs and contribute to life-long maintenance or repair of the tissue (Asakura and Rudnicki, 2002; Montanaro et al., 2003). Quiescence of CSPs was confirmed by PY staining. Stem cell niches play a pivotal role in controlling the self-renewal and differentiation of stem cells (for review see Moore and Lemischka, 2006). Niches consist of stem cells, niche stromal cells, and extracellular matrix, and the interaction between stem cells and the cellular microenvironments through adhesion molecules is important, as are paracrine factors. Bcrp1-positive cells in the heart coexpressed CD29 and

N-cadherin on their cell surface and were located in the interstitial space and perivascular area. Although the niche stroma cells for cardiac Bcrp1-positive cells were not specified in this study, the fact that most Bcrp1-positive cells existed in the perivascular area suggests that pericytes or adventitial mesenchymal cells may be a component of the stem cell niches. During the preparation of this manuscript, Urbanek et al. (2006) reported that c-kit–positive cardiac stem cells and lineage-committed cells are clustered together, forming their niches in adult mouse heart. In their paper, $\alpha 4\beta 1$ integrin–mediated adhesion to laminin and fibronectin, as well as E- and N-cadherin–mediated cell–cell communications are supposed to be the fundamental structure of the cardiac stem cell niches. Some groups have reported that the frequency of cardiac stem cell clusters, including MDR1-positive cells, is inversely related to the hemodynamic load sustained by the anatomical regions of the heart; they accumulate in the atria and apex and are less numerous at the base and mid portion of the left ventricle (Leri et al., 2005). However, the frequency of CD31-negative/Bcrp1-positive cells in neonatal hearts did not show significant difference in the anatomical regions in this study. The reason for this discordant result may be that the left ventricle of neonatal hearts is under less hemodynamic load than that of adult hearts.

Intravenously transplanted CSPs were trapped in the lung and spleen, but redistributed in heart, liver, and skeletal muscle. CSPs in the heart were localized in the basal membrane between the myocardium and expressed CD29 on their cell surface, suggesting that CSPs penetrate the fenestrated endothelium, migrate into the basal lamina, and reside along with cardiomyocytes. Although some CSPs in liver and skeletal muscle expressed tissue-specific proteins such as albumin and desmin, respectively, transplanted CSPs in the normal heart did not express cardiac contractile proteins. It has been reported that transplanted bone marrow cells fuse with hepatocytes and skeletal muscle and regenerate the tissues (Camargo et al., 2003;

Corbel et al., 2003; Vassilopoulos et al., 2003; Wang et al., 2003). Therefore, highly fusogenic hepatocytes and myotubes may fuse with transplanted CSPs and express differentiated marker proteins, whereas CSPs homing to the heart may not fuse with cardiomyocytes, and thus maintain stem or progenitor status.

Tissue damage, such as total body irradiation or chemotherapy, leads to secretion of chemokines and cytokines and facilitates hematopoietic stem cell migration and repopulation (Lapidot et al., 2005). Torrente et al. (2003) reported that skeletal muscle–derived stem cells home and migrate to the perivascular space of a damaged muscle of *mdx* mice after intravenous transplantation, and that the molecules involved in this process are L-selectin and mucosal addressin cell adhesion molecule-1. CSPs distributed in lung, spleen, liver, and skeletal muscle, but did not home specifically to the normal heart tissue. However, CSPs infused into rats with cryoinjured hearts homed in the heart, suggesting that the factors inducing migration and homing of stem cells may be released from injured heart. Further studies are necessary to understand the molecular mechanisms of differentiation, expansion, and migration of cardiac stem cells.

Materials and methods

Cell preparation and reagents
Neonatal Wistar rats and wild-type mice (C57BL/6) were purchased from Takasugi Experimental Animal Supply Co. LTD. Neonatal and adult GFP transgenic rats were purchased from Japan SLC, Inc. (Ito et al., 2001). All protocols were approved by the Institutional Animal Care and Use Committee of Chiba University. Cardiomyocytes of neonatal rats were prepared as previously described (Komuro et al., 1990). Rabbit anti–mouse Bcrp1 antibody was provided by S. Takeda (National Center of Neurology and Psychiatry, Tokyo, Japan; Uezumi et al., 2006). Other antibodies used in these studies are listed in Table I. Other reagents that are not specified were obtained from Sigma-Aldrich.

Isolation of CSPs and Pyronin Y staining
Cardiac cells were resuspended at the density of 1.0×10^6 cells/ml in PBS with 3% FBS. The cells were incubated in 1 μg/ml Hoechst 33342 dye for 60 min at 37°C in the dark, with or without 50 μM verapamil. After the

Table I. **Primary antibodies used**

Antibodies	Clone	Conjugate Used	Source
anti-CD31	TLD-3A12	PE	BD Biosciences
anti-CD45	OX-1	PE	BD Biosciences
anti-CD29	HMβ1-1	Unconjugated FITC	BD Biosciences
anti-cTnT	RV-C2	Unconjugated	German Resource Centre for Biological Material
anti-ANF	polyclonal	Unconjugated	Peninsula Laboratories
anti-GATA4	polyclonal	Unconjugated	Santa Cruz Biotechnology, Inc.
anti–MLC-2v	F109.3E1	Unconjugated	BioCytex
anti–β-galactosidase	polyclonal	Unconjugated	CHEMICON International, Inc.
anti-vimentin	monoclonal	Unconjugated	PROGEN
anti-vWF	polyclonal	Unconjugated	DAKO Cytomation
anti-SMA	1A4	Unconjugated	DAKO Cytomation
anti-calponin	CALP	Unconjugated	DAKO Cytomation
anti-desmin	polyclonal	Unconjugated	DAKO Cytomation
anti–N-cadherin	3B9	Unconjugated	Zymed Laboratories
anti-SA	EA-53	Unconjugated	Sigma-Aldrich
anti-GFP	monoclonal	Unconjugated	Marine Biological Laboratory
anti-GFP	polyclonal	Unconjugated	Marine Biological Laboratory
anti-albumin	polyclonal	Unconjugated	Intercell Technologies

incubation, cells were analyzed for Hoechst 33342 dye efflux by EPICS ALTRA flow cytometric analysis (Beckman Coulter). Before analysis, 2 µg/ml of propidium iodide was added to distinguish live cells from dead cells. Hoechst 33342 dye was excited at 350 nm using UV laser. Fluorescent emission was detected through 450-nm BP (Hoechst blue) and 675-nm LP (Hoechst red) filters, respectively. Propidium iodide in cells was excited at 488 nm, and fluorescence emission was detected through a 610-nm BP filter. For cell surface marker analysis, the cells were incubated with phycoerythrin (PE)-conjugated anti-CD45 antibody, PE-conjugated anti-CD31 antibody, or FITC-conjugated anti-CD29 antibody for 10 min on ice and washed with PBS supplemented with 3% FBS. The procedures for mouse bone marrow SP cells and PY staining were previously described (Goodell et al., 1996; Arai et al., 2004).

Cell culture
CSPs were cultured on gelatin-coated dishes with Iscove's Modified Dulbecco's Medium supplemented with 10% FBS. 24 h after seeding, the cells were treated with 10 pg/ml TSA or 100 nM of OT (both Sigma-Aldrich) for 72 h.

CSP transplantation of cryoinjured heart model
Male Wistar rats were anesthetized with 50 mg/kg ketamine i.p. and xylidine (10 mg/kg, i.p.) and a 6-mm aluminum rod, which was cooled to –190°C by immersion in liquid nitrogen, applied to the left ventricular free wall to produce cryoinjury, after the tail vein injection of 3×10^5 CSPs or CMPs derived from neonatal GFP transgenic into syngenic wild-type adult rats (CSP transplantation, $n = 3$; CMP transplantation, $n = 3$). As control groups, normal rats, which were subjected to the injection of 3×10^5 of CSPs ($n = 3$) or CMP ($n = 3$) were prepared. 4 wk after injection, rats were killed and lung, spleen, liver, skeletal muscle, and heart were fixed according to the periodate-lysine-paraformaldehyde fixative methods and snap-frozen in liquid nitrogen.

Immunocytochemistry and histochemistry
Cells were fixed with 4% paraformaldehyde and preblocked with PBS containing 2% donkey serum, 2% BSA, and 0.2% NP-40 for 30 min.

Primary antibodies in PBS containing 2% donkey serum, 2% BSA, and 0.1% NP-40 were applied overnight at 4°C. FITC-, Cy3-, or Cy5-conjugated secondary antibodies were applied to visualize expression of specific proteins. Nuclear staining was performed with TOPRO-3 (Invitrogen). To detect expression of Bcrp1, fresh isolated cells were fixed in methanol/ethanol (1:1) for 1 min, and the cells were incubated with rabbit anti–mouse Bcrp1 antibodies for 2 h at room temperature. After washing three times with PBS containing 2% donkey serum, the secondary antibody was added for 1 h.

6-µm cryostat sections of fresh-frozen or fixed rat heart were prepared. Fresh-frozen sections were fixed with 1% formaldehyde for 15 min at room temperature. Blocking and staining procedures were performed according to the protocol described in the previous paragraph. Confocal images were acquired at room temperature using a microscope (Radiance 2000; Bio-Rad Laboratories) with Plan Apo 60×/1.40 NA oil immersion objective (Nikon) and Laser Sharp 2000 confocal software (Bio-Rad Laboratories). For Fig. 1 B (d and e), Fig. 5 B (a and b), Fig. S1 A (a and c), and Fig. S3 A (a–f), Axioscop 2 Plus (Carl Zeiss MicroImaging, Inc.) with Plan-NEOFLUAR 100×/1.30 NA oil immersion and 40×/0.75 NA objectives (Carl Zeiss MicroImaging, Inc.).

RNA extraction and RT-PCR analysis
SP cells were isolated from cardiac cells using EPICS ALTRA flow cytometric sorting. Total RNA was obtained from SP cells, TSA-treated SP cells, and the neonatal rat heart by RNA-Bee reagent (TEL-TEST). RT-PCR was performed using 0.1 mg of total RNA. For semiquantitative analysis, reverse transcribed products were pooled and fivefold serial dilutions were used for PCR. PCR was performed in a reaction volume of 20 µl with 200 nM deoxynucleoside triphosphates, 500 nM each of sense and antisense primers, and 2.5 U/100 µl Taq polymerase (Roche). Every PCR condition was confirmed to be within the linear range and within semiquantitative range for these specific genes and primer pairs. The primers used in this study and the PCR conditions are described in Table II. To confirm that the obtained bands were not derived from contaminated genomic DNA, a negative experiment was done for each sample without reverse transcriptase

Table II. **PCR primers and PCR conditions**

Primer	Product Size	Annealing Temperature
	bp	°C
β myosin heavy chain		
5'-GCCAACACCAACCTGTCCAAGTTC-3'	205	66
5'-TGCAAAGGCTCCAGGTCTGAGGGC-3'		
MLC-2v		
5'-GCCAAGAAGCGGATAGAAGG-3'	499	55
5'-CTGTGGTTCAGGGCTCAGTC-3'		
Nkx-2.5		
5'-CAGTGGAGCTGGACAAAGCC-3'	216	55
5'-TAGCGACGGTTCTGGAATTT-3'		
GATA4		
5'-CTGTCATCTCACTATGGGCA-3'	275	60
5'-CCAAGTCCGAGCAGGAATTT-3'		
MEF2C		
5'-GGCCATGGTACACCGAGTACAACGAGC-3'	401	62
5'-GGGGATCCCTGTGTTACCTGCACTTGG-3'		
ALP		
5'-TTGAAACTCCAAAAGCTCAACACCA-3'	450	62
5'-TCTCGTTATCCGAGTACCAGTCCC-3'		
Bcrp1		
5'-CCATAGCCACAGGCCAAAGT-3'	327	56
5'-GGGCCACATGATTCTTCCAC-3'		
GAPDH		
5'-TTCTACCCACGGCAAGTTCAA-3'	470	63
5'-GGATGACCTTGCCCACAGC-3'		
β-actin		
5'-GGACCTGGCTGGCCGGGACC-3'	583	60
5'-GCGGTGCACGATGGAGGGGC-3'		

before PCR. Amplified samples were electrophoresed on 2% agarose gels and stained with ethidium bromide. For semiquantitative RT-PCR analysis, PCR was performed on undiluted cDNA and on fivefold serial dilutions of cDNA, and the intensity of the ethidium bromide–stained bands was quantified using the Image program (Wayne Rasband, National Institutes of Health). Diluted pools showing the same intensity for β-actin were used for further PCR and quantification of Nkx-2.5 gene expression.

Differentiation cultures for osteocytes and adipocytes
The protocol for osteocyte- and adipocyte-induction was previously described (Matsuura et al., 2004). Alkaline phosphatase staining (leukocyte alkaline phosphatase assay kit) was used to examine the differentiation of osteocytes. For detection of accumulated oil droplets, Oil Red O staining was performed followed by nuclear hematoxylin counterstaining.

Statistical analysis
The significance of differences among mean values was determined by t test. P values were corrected for multiple comparisons by the Bonferoni correction. The accepted level of significance was $P < 0.05$.

Online supplemental material
Fig. S1 shows the osteogenic and adipogenic differentiation of CSPs. Fig. S2 shows the fine sarcomeric patterns of OT- and TSA-induced CSP-derived cardiomyocytes. Live images of beating cells were taken with an inverted microscope (Carl Zeiss MicroImaging, Inc.) equipped with chilled charge-coupled device camera (Hamamatsu) using I-O DATA Videorecorder software. Online supplemental material is available at http://www.jcb.org/cgi/content/full/jcb.200603014/DC1.

References

Arai, F., A. Hirao, M. Ohmura, H. Sato, S. Matsuoka, K. Takubo, K. Ito, G.Y. Koh, and T. Suda. 2004. Tie2/angiopoietin-1 signaling regulates hematopoietic stem cell quiescence in the bone marrow niche. *Cell*. 118:149–161.

Asakura, A., and M.A. Rudnicki. 2002. Side population cells from diverse adult tissues are capable of in vitro hematopoietic differentiation. *Exp. Hematol*. 30:1339–1345.

Asakura, A., P. Seale, A. Girgis-Gabardo, and M.A. Rudnicki. 2002. Myogenic specification of side population cells in skeletal muscle. *J. Cell. Biol*. 159:123–134.

Beltrami, A.P., L. Barlucchi, D. Torella, M. Baker, F. Limana, S. Chimenti, H. Kasahara, M. Rota, E. Musso, K. Urbanek, et al. 2003. Adult cardiac stem cells are multipotent and support myocardial regeneration. *Cell*. 114:763–776.

Camargo, F.D., R. Green, Y. Capetanaki, K.A. Jackson, and M.A. Goodell. 2003. Single hematopoietic stem cells generate skeletal muscle through myeloid intermediates. *Nat. Med*. 9:1520–1527.

Cai, C.L., X. Liang, Y. Shi, P.H. Chu, S.L. Pfaff, J. Chen, and S. Evans. 2003. Isl1 identifies a cardiac progenitor population that proliferates prior to differentiation and contributes a majority of cells to the heart. *Dev. Cell*. 6:877–889.

Colucci, W.S. 1997. Molecular and cellular mechanisms of myocardial failure. *Am. J. Cardiol*. 80:15L–25L.

Corbel, S.Y., A. Lee, L. Yi, J. Duenas, T.R. Brazelton, H.M. Blau, and F.M. Rossi. 2003. Contribution of hematopoietic stem cells to skeletal muscle. *Nat. Med*. 9:1528–1532.

Eisenberg, C.A., R.G. Gourdie, and L.M. Eisenberg. 1997. Wnt-11 is expressed in early avian mesoderm and required for the differentiation of the quail mesoderm cell line QCE-6. *Development*. 124:525–536.

Gimpl, G., and F. Fahrenholz. 2001. The oxytocin receptor system: structure, function, and regulation. *Physiol. Rev*. 81:629–683.

Gonzalez-Reyes, A. 2003. Stem cells, niches and cadherins: a view from *Drosophila*. *J. Cell Sci*. 116:949–954.

Goodell, M.A., K. Brose, G. Paradis, A.S. Conner, and R.C. Mulligan. 1996. Isolation and functional properties of murine hematopoietic stem cells that are replicating in vivo. *J. Exp. Med*. 183:1797–1806.

Goodell, M.A., M. Rosenzweig, H. Kim, D.F. Marks, M. DeMaria, G. Paradis, S.A. Grupp, C.A. Sieff, R.C. Mulligan, and R.P. Johnson. 1997. Dye efflux studies suggest that hematopoietic stem cells expressing low or undetectable levels of CD34 antigen exist in multiple species. *Nat. Med*. 3:1337–1345.

Gussoni, E., Y. Soneoka, C.D. Strickland, E.A. Buzney, M.K. Khan, A.F. Flint, L.M. Kunkel, and R.C. Mulligan. 1999. Dystrophin expression in the mdx mouse restored by stem cell transplantation. *Nature*. 401:390–394.

Gutkowska, J., M. Jankowski, C. Lambert, S. Mukaddam-Daher, H.H. Zingg, and S.M. McCann. 1997. Oxytocin releases atrial natriuretic peptide by combining with oxytocin receptors in the heart. *Proc. Natl. Acad. Sci. USA*. 94:11704–11709.

Hassig, C.A., and S.L. Schreiber. 1997. Nuclear histone acetylases and deacetylases and transcriptional regulation: HATs off to HDACs. *Curr. Opin. Chem. Biol*. 1:300–308.

Hierlihy, A.M., P. Seale, C.G. Lobe, M.A. Rudnicki, and L.A. Megeney. 2002. The post-natal heart contains a myocardial stem cell population. *FEBS Lett*. 530:239–243.

Hsieh, J., K. Nakashima, T. Kuwabara, E. Mejia, and F.H. Gage. 2004. Histone deacetylase inhibition-mediated neuronal differentiation of multipotent adult neural progenitor cells. A. *Proc. Natl. Acad. Sci. USA*. 101:16659–16664.

Iijima, Y., T. Nagai, M. Mizukami, K. Matsuura, T. Ogura, H. Wada, H. Toko, H. Akazawa, H. Takano, H. Nakaya, and I. Komuro. 2003. Beating is necessary for transdifferentiation of skeletal muscle-derived cells into cardiomyocytes. *FASEB J*. 17:1361–1363.

Ito, T., A. Suzuki, E. Imai, M. Okabe, and M. Hori. 2001. Bone marrow is a reservoir of repopulating mesangial cells during glomerular remodeling. *J. Am. Soc. Nephrol*. 12:2625–2635.

Jackson, K.A., S.M. Majka, H. Wang, J. Pocius, C.J. Hartley, M.W. Majesky, M.L. Entman, L.H. Michael, K.K. Hirschi, and M.A. Goodell. 2001. Regeneration of ischemic cardiac muscle and vascular endothelium by adult stem cells. *J. Clin. Invest*. 107:1395–1402.

Jankowski, M., F. Hajjar, S.A. Kawas, S. Mukaddam-Daher, G. Hoffman, S.M. McCann, and J. Gutkowska. 1998. Rat heart: a site of oxytocin production and action. *Proc. Natl. Acad. Sci. USA*. 95:14558–14563.

Jankowski, M., B. Danalache, D. Wang, P. Bhat, F. Hajjar, M. Marcinkiewicz, J. Paquin, S.M. McCann, and J. Gutkowska. 2004. Oxytocin in cardiac ontogeny. *Proc. Natl. Acad. Sci. USA*. 101:13074–13079.

Koipally, J., A. Renold, J. Kim, and K. Georgopoulos. 1999. Repression by Ikaros and Aiolos is mediated through histone deacetylase complexes. *EMBO J*. 18:3090–3100.

Komuro, I., T. Kaida, Y. Shibazaki, M. Kurabayashi, Y. Katoh, E. Hoh, F. Takaku, and Y. Yazaki. 1990. Stretching cardiac myocytes stimulates protoooncogene expression. *J. Biol. Chem*. 265:3595–3598.

Lapidot, T., A. Dar, and O. Kollet. 2005. How do stem cells find their way home? *Blood*. 106:1901–1910.

Laugwitz, K.L., A. Moretti, J. Lam, P. Gruber, Y. Chen, S. Woodard, L.Z. Lin, C.L. Cai, M.M. Lu, M. Reth, et al. 2005. Postnatal isl1+ cardioblasts enter fully differentiated cardiomyocyte lineages. *Nature*. 433:647–653.

Legube, G., and D. Trouche. 2003. Regulating histone acetyltransferases and deacetylases. *EMBO Rep*. 4:944–947.

Leri, A., J. Kajstura, and P. Anversa. 2005. Cardiac stem cells and mechanisms of myocardial regeneration. *Physiol. Rev*. 85:1373–1416.

Linke, A., P. Muller, D. Nurzynska, C. Casarsa, D. Torella, A. Nascimbene, C. Castaldo, S. Cascapera, M. Bohm, F. Quaini, et al. 2005. Stem cells in the dog heart are self-renewing, clonogenic, and multipotent and regenerate infarcted myocardium, improving cardiac function. *Proc. Natl. Acad. Sci. USA*. 102:8966–8971.

Makino, S., K. Fukuda, S. Miyoshi, F. Konishi, H. Kodama, J. Pan, M. Sano, T. Takahashi, S. Hori, H. Abe, et al. 1999. Cardiomyocytes can be generated from marrow stromal cells in vitro. *J. Clin. Invest*. 103:697–705.

Marks, P.A., T. Miller, and V.M. Richon. 2003. Histone deacetylases. *Curr. Opin. Pharmacol*. 3:344–351.

Martin, C.M., A.P. Meeson, S.M. Robertson, T.J. Hawke, J.A. Richardson, S. Bates, S.C. Goetsch, T.D. Gallardo, and D.J. Garry. 2004. Persistent expression of the ATP-binding cassette transporter, Abcg2, identifies cardiac SP cells in the developing and adult heart. *Dev. Biol*. 265:262–275.

Matsuura, K., T. Nagai, N. Nishigaki, T. Oyama, J. Nishi, H. Wada, M. Sano, H. Toko, H. Akazawa, T. Sato, et al. 2004. Adult cardiac Sca-1-positive cells differentiate into beating cardiomyocytes. *J. Biol. Chem*. 279:11384–11391.

Montanaro, F., K. Liadaki, J. Volinski, A. Flint, and L.M. Kunkel. 2003. Skeletal muscle engraftment potential of adult mouse skin side population cells. *Proc. Natl. Acad. Sci. USA*. 100:9336–9341.

Moore, K.A., and I.R. Lemischka. 2006. Stem cells and their niches. *Science*. 311:1880–1885.

Naito, A.T., A. Tominaga, M. Oyamada, Y. Oyamada, I. Shiraishi, K. Monzen, I. Komuro, and T. Takamatsu. 2003. Early stage-specific inhibitions of cardiomyocyte differentiation and expression of Csx/Nkx-2.5 and GATA-4 by phosphatidylinositol 3-kinase inhibitor LY294002. *Exp. Cell Res.* 291:56–69.

Oh, H., S.B. Bradfute, T.D. Gallardo, T. Nakamura, V. Gaussin, Y. Mishina, J. Pocius, L.H. Michael, R.R. Behringer, D.J. Garry, et al. 2003. Cardiac progenitor cells from adult myocardium: homing, differentiation, and fusion after infarction. *Proc. Natl. Acad. Sci. USA*. 100:12313–12318.

Pandur, P., M. Lasche, L.M. Eisenberg, and M. Kuhl. 2002. Wnt-11 activation of a non-canonical Wnt signalling pathway is required for cardiogenesis. *Nature*. 418:636–641.

Paquin, J., B.A. Danalache, M. Jankowski, S.M. McCann, and J. Gutkowska. 2002. Oxytocin induces differentiation of P19 embryonic stem cells to cardiomyocytes. *Proc. Natl. Acad. Sci. USA*. 99:9550–9555.

Pfister, O., F. Mouquet, M. Jain, R. Summer, M. Helmes, A. Fine, W.S. Colucci, and R. Liao. 2005. CD31- but Not CD31+ cardiac side population cells exhibit functional cardiomyogenic differentiation. *Circ. Res.* 97:52–61.

Schultheiss, T.M., J.B. Burch, and A.B. Lassar. 1997. A role for bone morphogenetic proteins in the induction of cardiac myogenesis. *Genes Dev.* 11:451–462.

Shimano, K., M. Satake, A. Okaya, J. Kitanaka, N. Kitanaka, M. Takemura, M. Sakagami, N. Terada, and T. Tsujimura. 2003. Hepatic oval cells have the side population phenotype defined by expression of ATP-binding cassette transporter ABCG2/BCRP1. *Am. J. Pathol.* 163:3–9.

Sugi, Y., and J. Lough. 1995. Activin-A and FGF-2 mimic the inductive effects of anterior endoderm on terminal cardiac myogenesis in vitro. *Dev. Biol.* 168:567–574.

Summer, R., D.N. Kotton, X. Sun, B. Ma, K. Fitzsimmons, and A. Fine. 2003. Side population cells and Bcrp1 expression in lung. *Am. J. Physiol. Lung Cell. Mol. Physiol.* 285:L97–L104.

Tamaki, T., A. Akatsuka, Y. Okada, Y. Matsuzaki, H. Okano, and M. Kimura. 2003. Growth and differentiation potential of main- and side-population cells derived from murine skeletal muscle. *Exp. Cell Res.* 291:83–90.

Tomita, Y., K. Matsumura, Y. Wakamatsu, Y. Matsuzaki, I. Shibuya, H. Kawaguchi, M. Ieda, S. Kanakubo, T. Shimazaki, S. Ogawa, et al. 2005. Cardiac neural crest cells contribute to the dormant multipotent stem cell in the mammalian heart. *J. Cell Biol.* 170:1135–1146.

Torrente, Y., G. Camirand, F. Pisati, M. Belicchi, B. Rossi, F. Colombo, M. El Fahime, N.J. Caron, A.C. Issekutz, G. Constantin, et al. 2003. Identification of a putative pathway for the muscle homing of stem cells in a muscular dystrophy model. *J. Cell Biol.* 162:511–520.

Towbin, J.A., and N.E. Bowles. 2002. The failing heart. *Nature*. 415:227–233.

Uezumi, A., K. Ojima, S. Fukada, M. Ikemoto, S. Masuda, Y. Miyagoe-Suzuki, and S. Takeda. 2006. Functional heterogeneity of side population cells in skeletal muscle. *Biochem. Biophys. Res. Commun.* 341:864–873.

Urbanek, K., D. Cesselli, M. Rota, A. Nascimbene, A. De Angelis, T. Hosoda, C. Bearzi, A. Boni, R. Bolli, J. Kajstura, et al. 2006. Stem cell niches in the adult mouse heart. *Proc. Natl. Acad. Sci. USA*. 103:9226–9231.

Vassilopoulos, G., P.R. Wang, and D.W. Russell. 2003. Transplanted bone marrow regenerates liver by cell fusion. *Nature*. 422:901–904.

Ventura, C., and M. Maioli. 2000. Opioid peptide gene expression primes cardiogenesis in embryonal pluripotent stem cells. *Circ. Res.* 87:189–194.

Ventura, C., E. Zinellu, E. Maninchedda, and M. Maioli. 2003. Dynorphin B is an agonist of nuclear opioid receptors coupling nuclear protein kinase C activation to the transcription of cardiogenic genes in GTR1 embryonic stem cells. *Circ. Res.* 92:623–629.

Wang, X., H. Willenbring, Y. Akkari, Y. Torimaru, M. Foster, M. Al-Dhalimy, E. Lagasse, M. Finegold, S. Olson, and M. Grompe. 2003. Cell fusion is the principal source of bone-marrow-derived hepatocytes. *Nature*. 422:897–901.

Wilson, A., M.J. Murphy, T. Oskarsson, K. Kaloulis, M.D. Bettess, G.M. Oser, A.C. Pasche, C. Knabenhans, H.R. Macdonald, and A. Trumpp. 2004. c-Myc controls the balance between hematopoietic stem cell self-renewal and differentiation. *Genes Dev.* 18:2747–2763.

Xu, C., S. Police, N. Rao, and M.K. Carpenter. 2002. Characterization and enrichment of cardiomyocytes derived from human embryonic stem cells. *Circ. Res.* 91:501–508.

Zhang, J., C. Niu, L. Ye, H. Huang, X. He, W.G. Tong, J. Ross, J. Haug, T. Johnson, J.Q. Feng, et al. 2003. Identification of the haematopoietic stem cell niche and control of the niche size. *Nature*. 425:836–841.

Zhou, S., J.D. Schuetz, K.D. Bunting, A.M. Colapietro, J. Sampath, J.J. Morris, I. Lagutina, G.C. Grosveld, M. Osawa, H. Nakauchi, and B.P. Sorrentino. 2001. The ABC transporter Bcrp1/ABCG2 is expressed in a wide variety of stem cells and is a molecular determinant of the side-population phenotype. *Nat. Med.* 7:1028–1034.